306 © *1983 The Chemical Society of Japan* *Bull. Chem. Soc. Jpn.*, ***56***, *306—313 (1983)* [Vol. 56, No. 1

Restricted Rotation Involving the Tetrahedral Carbon. XLV. Appearance of a Maximum in the Rotational Barriers of 9-(1,1-Dimethyl-2-phenylethyl)triptycenes at a Medium-sized *peri*-Substituent[1)]

Gaku Yamamoto, Masahiko Suzuki, and Michinori Ōki*

Department of Chemistry, Faculty of Science, The University of Tokyo, Bunkyo-ku, Tokyo 113

(Received August 10, 1982)

Rotational isomers of seven *peri*-substituted 9-(1,1-dimethyl-2-phenylethyl)triptycene derivatives were stereoselectively synthesized and classical kinetics on rotational isomerization were studied. While compounds with relatively small *peri*-substituents (F and OCH_3) showed higher barriers than the *peri*-unsubstituted one, the *peri*-chloro compound had almost the same barrier with and those carrying bulkier *peri*-substituents (Br, CH_3, and CF_3) showed lower barriers than the *peri*-unsubstituted one. These apparently anomalous phenomena may be explained in terms of large molecular deformation of these highly congested compounds.

We have shown by NMR spectroscopy that 9-substituted triptycene derivatives constitute an excellent model system in the investigation of rotational isomerism about a single bond.[2)] The compounds have high barriers to rotation about the bridgehead-to-substituent bond because of the rigidity of the triptycene skeleton. Thus, even a methyl group shows restricted rotation on the NMR time scale in some 9-methyltriptycene derivatives.[3)]

Bulkiness of the 9-substituent is the largest factor governing the height of the barrier. Thus, 9-*t*-alkyltriptycenes have high rotational barriers enough to give rise to rotational isomers isolable at room temperature (atropisomers).[4)]

Substitution at *peri*-positions (1-, 8-, and 13-positions) also has a large influence on the barrier. While 9-benzyltriptycenes carrying one *peri*-substituent showed the rotational barrier of *ca.* 12 kcal mol^{-1} (1 cal=4.184 J),[5)] a triply *peri*-substituted 9-benzyltriptycene could give rise to stable atropisomers with the barrier of 25.3 kcal mol^{-1}.[6)] Influence of the nature (mainly steric) of *peri*-substituents on the rotational barrier has been studied in some of singly *peri*-substituted 9-alkyl(or aralkyl)triptycenes. When the 9-substituent is a primary or a secondary alkyl group, the barrier increases with the bulkiness of the *peri*-substituent.[3,7,8)] This tendency can be easily understood if one accepts that the effect of steric crowding due to the *peri*-substitution should be larger in the transition state than in the ground state.

In the case of 9-(1-cyano or 1-methoxycarbonyl-1-methylethyl)triptycene, however, introduction of a chloro or a methyl group into a *peri*-position was found to decrease the rotational barrier, the clear explanation remaining to be solved.[9)]

In order to see if this phenomenon is generally observed in 9-*t*-alkyltriptycene derivatives, and also to get a deeper insight into the origin of the phenomena by investigating the effects of some other *peri*-substituents, we studied the rotational barriers of a variety of *peri*-substituted 9-(1,1-dimethyl-2-phenylethyl)triptycene derivatives **2**—**8**.[10)] The results are presented in this paper. The choice of this particular system is based on the following reasons. Firstly, the 9-substituent has no polar bond which might have special interaction with *peri*-substituents. Secondly, similarity in bulkiness between methyl and benzyl groups might not cause a large shift of the rotational equilibrium from the statistical value, which would make kinetic measurements easy. Thirdly, we previously reported on the synthesis of and the rotational barrier in the *peri*-unsubstituted derivative **1**.[4)]

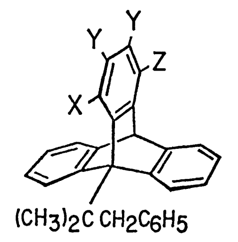

	X	Y	Z
1	H	Cl	H
2	F	H	H
3	OCH_3	H	OCH_3
4	Cl	H	H
5	Cl	H	Cl
6	Br	H	H
7	CH_3	H	CH_3
8	CF_3	H	H

Results

Syntheses. Triptycenes investigated were synthesized by the reactions of 9-(1,1-dimethyl-2-phenylethyl)-anthracene (**9**) with benzynes **10** and **11**. The benzyne (**11a**) was generated by decomposition of 2,6-difluorophenyllithium prepared from *m*-difluorobenzene and butyllithium.[11)] The other benzynes were generated by decomposition of 3- or 3,6-substituted 2-diazoniobenzoates prepared from the corresponding anthranilic acids and isopentyl nitrite. The triptycenes formed existed exclusively in the *ap* atropisomer in accordance with the stereoselectivity previously found in the case of **1**. Thus, the atropisomer is selectively formed in which the bulkier group in the 9-substituent assumes the antiperiplanar position to the benzeno bridge derived from the benzyne.[4)] In the reactions of **9** with benzynes **11**, the regioisomeric 4-substituted triptycenes were formed in addition to the desired 1-substituted ones. Identification of the regioisomers was made by the chemical shifts of the bridgehead protons: those of 1-substituted derivatives appeared at δ 5.20—5.27, while those of 4-substituted ones appeared at a lower field because of the anisotropic and/or steric compression effects of the 4-substituent. The ratio of formation of 1- *vs.* 4-substituted compounds were as follows: 5.0 for **2**/**2′**, 1.3 for **4**/**4′**, 1.0 for **6**/**6′** and **8**/**8′**. Preferred formation of the more crowded regioisomers may be apparently anomalous, but is not unprecedented.[12)] Separation of the two regioisomers was successfully made by chromatography for **4**/**4′**, **6**/**6′**, and **8**/**8′**pairs. In the case of the fluoro derivatives (**2**/**2′**), the separation was extremely difficult, and the pure sample of

2 was obtained only in a minute amount. Therefore, synthesis of **2** by another route was explored. 9-(1,1-Dimethyl-2-phenylethyl)-1-fluoroanthracene (**14**) was prepared by the reaction of 1,1-dimethyl-2-phenylethylmagnesium chloride with 1-fluoroanthrone (**12**) followed by dehydration, and was treated with benzyne. In this reaction, the ±*sc* rotamer of **2** was stereoselectively obtained.

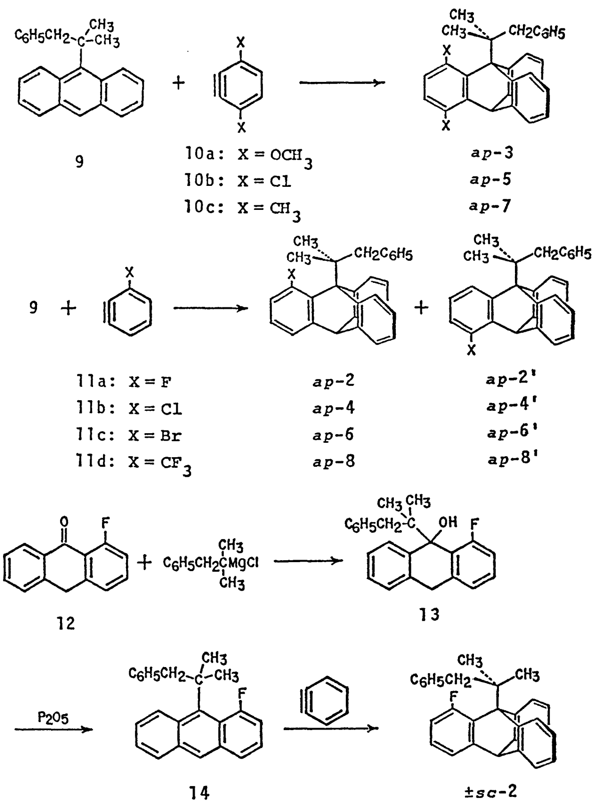

First choice for the isolation of the ±*sc* rotamers of compounds **3**—**8** was chromatography of the equilibrated rotamer mixture on alumina or silica-gel columns. In all cases the *ap* rotamers eluted slightly faster than the ±*sc*. The intrinsically small differences of the chromatographic properties between the rotamers as well as the unavolidable tailing of the bands of *ap* rotamers made isolation of the pure ±*sc* rotamers highly difficult, and the isolation in pure state was successful only for **3**. Secondly, separation by fractional recrystallization was tried but here again the situation was similar because the *ap* rotamers generally had better crystallizability than the ±*sc* rotamer and complete purification of the ±*sc* rotamer was made only for **7**. For compounds **4**, **5**, and **6**, the ±*sc*-enriched mixtures with the content of the *ap* rotamers of 20, 15, and 8%, respectively, were finally obtained. As for **8**, the ±*sc* rotamer was enriched only to 25%.

NMR Spectra. ^{1}H NMR spectral data for both rotamers of the triptycenes (**1**—**8**) are given in Table 1. As for the ±*sc* rotamers of **4**, **5**, **6**, and **8**, the data were obtained from the most enriched samples mentioned above by subtracting the signals due to the *ap* rotamers. Rotameric assignment was explicitly made from the NMR data. The *gem*-dimethyl groups of the *ap* rotamers are enantiotopic and appear as a singlet except for those of **2** and **8**, in which they appear as a doublet and a quartet, respectively, because of the long-range couplings with ^{19}F.[13] The methylene protons are singlets in all of the *ap* rotamers.

In the ±*sc* rotamers, the *gem*-dimethyl groups are *a priori* diastereotopic and actually are anisochronous. Positional assignment of the methyl signals was made as follows. In fluorine-containing compounds **2** and **8**, the signal exhibiting a large coupling with ^{19}F was assigned to the ±*sc*-methyl group, because the coupling should operate through-space under these circumstances and thus the protons located proximate to the ^{19}F nuclei show the coupling.[13]

Nuclear Overhauser effect (NOE) experiments allowed the definite assignment of the methyl signals for **3**—**6**. In any of the compounds, irradiation of the higher-field methyl signal enhanced the intensity of both of the *peri*-proton (8-H and 13-H) signals which appeared as two isolated multiplets at the lowest field region (δ 7.7—8.1). On the other hand, only the lower-field *peri*-proton signal showed enhancement of the intensity upon irradiation of the lower-field methyl signal. Therefore, the higher-field methyl signal is assigned to the *ap*-methyl group as shown in Table 1. In the ±*sc* rotamer of **1**, the 1-H signal appeared as a singlet at the lowest field (δ 8.03) together with two multiplets for 8-H and 13-H, and its intensity increased only when the higher-field methyl signal at δ 1.99 was irradiated, indicating that the signal should be assigned to the ±*sc*-methyl group. In ±*sc*-**7**, NOE experiments did not afford any information on the assignment because of the small chemical shift difference between the *gem*-dimethyl signals, and tentative assignment is given in Table 1.

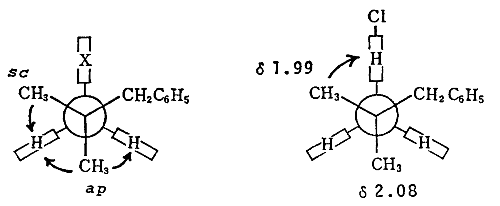

It is noticed that the *ap*-methyl signal appears at a lower field than that for the ±*sc*-methyl in **1** and **2**, but the reverse is observed in the other compounds. Roughly speaking, the ±*sc*-methyl signal shifts downfield and the *ap*-methyl upfield as the bulkiness of the *peri*-substituent increases. Large downfield shifts of the ±*sc*-methyl signals in **4**, **5**, **6**, and **8** must be due to the anisotropy and/or steric compression effects exerted by the *peri*-substituents. Upfield shift of the *ap*-methyl signals in these compounds may partly be ascribed to the molecular deformation, which is discussed in the later section.

The methylene protons of the ±*sc* rotamers are diastereotopic and appear as an AB-quartet except for those of ±*sc*-**8**, which give an apparent singlet in $CDCl_3$ because of the small chemical shift difference but show an AB-quartet signal (δ 4.11 and 4.24, J= 15.3 Hz) in a benzene solution.

Kinetics of Isomerization. A solution of a pure rotamer (±*sc* for **2**, *ap* for the others) in 1-chloronaphthalene was heated at a given temperature using

Table 1. ^{1}H NMR spectral data in $CDCl_3$ at 35 °C[a]

Compound	Atropisomer	*ap*-CH_3	±*sc*-CH_3	CH_2	10-H	1,4-Substituents
1[b]	*ap*		2.03	3.86	5.17	
	±*sc*	2.08	1.99	3.75 d, 3.89 d (14.6)	5.17	
2	*ap*		2.06 d (8.4[c])	3.90	5.27 d (1.8[a])	
	±*sc*	2.10	1.97 d (7.9[c])	3.77 d, 3.96 dd (14.4) (14.4 and 2.1[c])	5.27 d (1.7[c])	
3	*ap*		2.10	3.86	5.92	3.65, 3.79
	±*sc*	2.04	2.10	3.95 d, 4.22 d (14.4)	5.92	3.71, 3.81
4	*ap*		2.33	3.85	5.23	
	±*sc*	2.05	2.35	4.08 d, 4.57 d (15.0)	5.23	
5	*ap*		2.33	3.85	6.05	
	±*sc*	2.07	2.35	4.09 d, 4.50 d (15.3)	6.04	
6	*ap*		2.44	3.82	5.20	
	±*sc*	1.98	2.51	4.06 d, 4.86 d (15.2)	5.21	
7	*ap*		2.28	3.90	5.62	2.51, 2.61
	±*sc*	2.21[d]	2.25[d]	3.95 d, 4.27 d (16.0)	5.61	2.50, 2.75
8	*ap*		2.27 q (4.2[c])	3.75	5.25	
	±*sc*	1.85	2.40 q (4.6[c])	4.04[e]	5.25	

a) Chemieal shifts are shown in ppm downfield from internal tetramethylsilane. Signals are singlets unless otherwise stated; d: doublet, dd: doublet of doublets, q: quartet. In parentheses are coupling constants in Hz. b) Ref. 4. c) Long-range coupings with ^{19}F. d) Tentatively assigned. See text. e) Apparent singlet. An AB-quartet in benzene.

Table 2. Thermodynamic parameters for rotamer equilibrium[a]

Compound	ΔH kcal mol^{-1}	ΔS° [b] e.u.	ΔG°_{500} [b] kcal mol^{-1}	K_{500}	r_P[c] Å	r_C[d] Å
1[e]	0±0	0±0	0	2.0	1.2	1.20
2	0.20±0.62	−0.2±1.2	0.3	1.52	1.35	1.47
3	0.59±0.27	0.1±0.5	0.5	1.18	1.40	1.52
4	1.31±0.11	0.2±0.2	1.2	0.60	1.80	1.75
5	1.15±0.04	−0.2±0.1	1.3	0.57	1.80	1.75
6	1.35±0.03	−0.1±0.1	1.4	0.52	1.95	1.85
7	1.54±0.18	−0.2±0.4	1.6	0.39	2.0	1.97[f]
8	1.99±0.14	0.4±0.4	1.8	0.32		2.43[f]

a) Obtained from the data in Table 4. b) Degeneracy of ±*sc* rotamers is taken into account. c) Van der Waals radius according to Pauling: L. Pauling, "The Nature of the Chemical Bond," 3rd ed, Cornell University Press, New York (1960), p. 260. d) Van der Waals radius according to Charton: M. Charton, *J. Am. Chem. Soc.*, **91**, 615 (1969). e) Ref. 4. f) $(r_{v,\min}+r_{v,\max})/2$.

a boiling solvent bath. At appropriate intervals the sample was taken out of the bath and cooled to room temperature. NMR spectrum was taken to obtain the rotamer population. The ^{19}F signals were used for compounds **2** and **8**, and the *gem*-dimethyl proton signals for the others. Change in the rotamer population upon time obeyed the rate law for a first-order reversible reaction and the rate constant for the isomerization was obtained. The measurements were made at three to four temperatures over the range of 32—50 °C, and the Eyring kinetic parameters were calculated using least square analysis. In Table 4 are given the rate constants for the *ap*→±*sc* conversion by taking into account the degeneracy of the ±*sc* rotamers and the free energies of activation therefrom. Eyring parameters as well as free energies of activation and rate constants at 500 K are given in Table 3. The thermodynamic parameters were calculated from the equilibrium constants using the van't Hoff equation and are given in Table 2. Here also the degeneracy of the ±*sc* rotamers was taken into account.

TABLE 3. KINETIC PARAMETERS FOR ROTAMER ISOMERIZATION[a)]

Compound	ΔH^{*} / kcal mol^{-1}	ΔS^{*} / e.u.	ΔG^{*}_{500} / kcal mol^{-1}	k_{500} / s^{-1}	k_{rel}
1[b)]	35.5±2.2	−9.8±4.4	40.4	2.4×10^{-5}	20
2	41.2±1.3	−4.1±2.5	43.2	1.2×10^{-6}	1
3	42.6±0.2	0.2±0.3	42.5	2.8×10^{-6}	2
4	36.4±0.9	−8.0±1.9	40.4	2.1×10^{-5}	18
5	35.3±0.9	−9.2±1.9	39.9	3.6×10^{-5}	30
6	34.9±0.9	−8.7±1.9	39.2	7.2×10^{-5}	60
7	34.0±0.6	−8.7±1.2	38.4	1.8×10^{-4}	150
8	29.7±1.8	−8.0±4.5	33.8	1.9×10^{-2}	16000

a) Obtained from the data in Table 4. b) Ref. 4.

Discussion

General Consideration. Inspection of molecular models reveals that even in the simplest 9-*t*-alkyltriptycene, 9-*t*-butyltriptycene, the distance between a *peri*-hydrogen and the nearest methyl-hydrogen in the staggered conformation is only 1.5 Å, far shorter than the sum of the van der Waals radii, indicating that the compound itself is a highly crowded molecule. This suggests that introduction of a substituent into one of the *peri*-positions of the triptycyl skeleton should heavily affect the geometry and energy of the molecule.

As an energy barrier to internal rotation is the difference between the ground and the transition states, the influence of the *peri*-substitution on the energy barrier should be understood in terms of perturbation to the both states by the *peri*-substitution. Although the geometry and energy of the transition state can not be directly obtained experimentally, information about those of the ground state may be obtained from several sources.

X-Ray structural analysis of 9-*t*-butyl-1,2,3,4-tetrachlorotriptycene (**15**) revealed the presence of considerable molecular deformation.[14)] The most prominent features are the tiltings of the *t*-butyl and the *peri*-chloro groups away from each other (t-Bu–C_9–C_{1a}: 118.9°, C_{1a}–C_1–Cl: 125.4°) and the elongation of the C_9–C_{arom} bonds (especially C_9–C_{1a}: 1.603 Å) owing to steric compression.

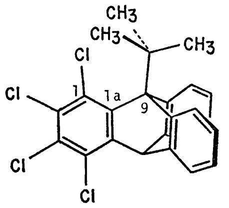

15

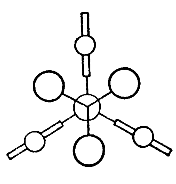

16

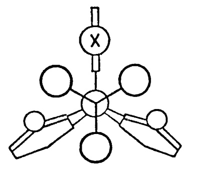

17

We now concentrate our attention to the tilting of the *t*-butyl–C_9 bond from the axis of the triptycene skeleton. The Newman projection of a *peri*-unsubsti-

TABLE 4. THERMODYNAMIC AND KINETIC DATA

$$ap \underset{k_{-1}}{\overset{2k_1}{\rightleftharpoons}} \pm sc \qquad K=2k_1/k_{-1}$$

Compound	Temp / °C	K	k_1 / s^{-1}	ΔG^{*} / kcal mol^{-1}
2	258	1.55	1.61×10^{-5}	43.3_4
	246	1.50	5.99×10^{-6}	43.3_6
	238	1.54	3.39×10^{-6}	43.2_5
	226.5	1.27	1.27×10^{-6}	43.2_3
3	259	1.22	3.90×10^{-5}	42.4_9
	246	1.21	1.38×10^{-5}	42.5_0
	239	1.18	8.03×10^{-6}	42.4_6
	220	1.17	1.49×10^{-6}	42.5_0
4	258[a)]	0.66		
	246[a)]	0.63		
	224	0.60	1.72×10^{-5}	40.4_4
	212	0.57	7.15×10^{-6}	40.2_8
	196.5	0.56	1.97×10^{-6}	40.1_7
	175	0.52	2.83×10^{-7}	40.0_2
5	225	0.57	3.16×10^{-5}	39.9_2
	212	0.55	1.21×10^{-5}	39.7_8
	189	0.52	1.71×10^{-6}	39.6_4
	175	0.50	5.54×10^{-7}	39.4_2
6	240[a)]	0.52		
	224.5	0.50	6.10×10^{-5}	39.2_3
	212	0.48	2.49×10^{-5}	39.0_8
	189	0.45	4.09×10^{-6}	38.8_4
	175	0.43	1.10×10^{-6}	38.8_1
7	219	0.38	1.02×10^{-4}	38.3_8
	212.5	0.37	6.55×10^{-5}	38.2_9
	187	0.34	8.61×10^{-6}	37.9_4
8	170[a)]	0.25		
	155[a)]	0.23		
	139.5	0.21	2.92×10^{-5}	32.9_9
	125.5	0.20	6.74×10^{-6}	33.0_0
	111.5	0.18	1.67×10^{-6}	32.8_8
	99.5	0.16	5.37×10^{-7}	32.6_7

a) Only the equilibrium constants are measured.

tuted 9-*t*-butyltriptycene along the *t*-butyl–C_9 bond is shown by **16**. If a substituent is introduced into one of the *peri*-positions, the steric repulsion between the *peri*-substituent and the *t*-butyl group should cause the tilting of the axis bond away from the *peri*-substituent. This feature can be represented by the Newman projection **17**. The degree of the tilting of the axis bond should become larger as the bulkiness of the *peri*-substituent increases. Similar molecular deformation should occur in 9-(1,1-dimethyl-2-phenylethyl)triptycenes.

^{1}H NMR spectral data in Table 1 indicate the tendency that the *ap*-methyl signal of the ±*sc* rotamer shifts upfield as the *peri*-substituent becomes bulkier. It is especially remarkable in the *peri*-trifluoromethyl derivative **8**, which shows the *ap*-methyl signal at δ 1.85. This trend seems compatible with the hypothesis that the molecular deformation becomes larger as the *peri*-substituent becomes bulkier. Thus, the larger tilting of the axis bond is rendering the *ap*-methyl group more susceptible to the shielding effect of the flanking benzene rings. Although less remarkable, similar trend is also observed in the methylene signals of the *ap* rotamers.

These features suggest that the ground state of a 9-(1,1-dimethyl-2-phenylethyl)triptycene becomes less and less stable as the *peri*-substituent becomes bulkier.

Rotational Equilibrium. Table 2 shows that the equilibrium is mainly governed by the enthalpy term ($\Delta H°$), the entropy term ($\Delta S°$) being very small. The equilibrium constant K for the *peri*-unsubstituted derivative **1** is a statistical value of 2.0, and this is thought reasonable if one admits that the 2,3-dichloro groups exert no appreciable effects as the first approximation. The $\Delta H°$ value gradually increases and the equilibrium constant at 500 K, K_{500}, monotonously decreases as the *peri*-substituent becomes bulkier. The bulkiness of the substituents is evaluated from the van der Waals radii of the groups. As for a methoxyl group, the radius of an oxygen atom may be used because the steric interaction of the *peri*-methoxyl group with the 9-substituent occurs primarily at the oxygen atom.

If one admits that a benzyl group is bulkier than a methyl, and that the degree of the tilting of the axis bond is similar between the rotamers, it is understood that the ±*sc* rotamer is more destabilized than the *ap* rotamer with the increasing bulkiness of the *peri*-substituent, in accordance with the observed tendency.

Rotational Barriers. Table 3 reveals a very interesting dependence of the rotational barrier on the *peri*-substituent. Introduction of a relatively small substituent, such as fluoro and methoxyl, raises the rotational barrier relative to the *peri*-unsubstituted compound **1**, which seems natural according to the normal chemical intuition. However, further increase in the bulkiness of the *peri*-substituent decreases the barrier. Thus, the *peri*-chloro derivatives **4** and **5** have almost the same barrier as **1**, and the *peri*-bromo (**6**) and the *peri*-methyl (**7**) compounds show lower barriers than **1**. Compound **8**, with the bulkiest *peri*-substituent examined, has a barrier 6.6 kcal mol^{-1} lower than that of **1**. Difference in free energies of activation between **2** and **8** amounts to 9.4 kcal mol^{-1}, which corresponds to the rate ratio of 16000 at 500 K. Drop in the barrier height upon introduction of a chloro or a methyl group into a *peri*-position is in accordance with our earlier observation in 9-(1-cyano or methoxycarbonyl-1-methylethyl)triptycenes,[9] and these phenomena seem to be general in 9-*t*-alkyltriptycenes.

As discussed above, the ground state should become less and less stable with the increasing bulkiness of the *peri*-substituent. The trend of the observed barrier heights implies that in the compounds with a bulky *peri*-substituent such as bromo, methyl, and trifluoromethyl, the transition state for rotation is destabilized to a lesser extent than the ground state and that this tendency becomes more remarkable as the *peri*-substituent becomes bulkier. In compounds **2** and **3** with a small *peri*-substituent the destabilization of the transition state exceeds that of the ground state.

It is noteworthy that in the compounds carrying a bulky *peri*-substituent the transition state is not destabilized to such an extent that is expected from the bulkiness of the *peri*-substituent. Consideration on the deformed model with the tilted axis bond mentioned above affords a transition state model which may partly explain the lesser stabilization of the transition state relative to the ground state, as described in the following sections.

For the sake of simplicity, we will discuss on the 9-*t*-butyl compounds, but the similar argument should apply to the 9-(1,1-dimethyl-2-phenylethyl) system. We now consider to rotate the *t*-butyl group around the tilted axis. Here we assume that both the triptycyl skeleton and the *t*-butyl group can be regarded as rigid rotors. The rotational itinerary can be shown by the Newman projections in Scheme 1. We notice that the eclipsing of a methyl in the *t*-butyl group with the *peri*-substituent or a *peri*-hydrogen does not occur simultaneously but sequentially at the three sites. Thus, while eclipsing of methyl A with the *peri*-substituent X occurs in the conformation **19**, that of methyls B and C with nearby *peri*-hydrogens is attained before and after **19**, in conformations **18** and **20** with the torsion angle of $\pm\theta$. Intervals of the maximal eclipsing at the three sites as expressed by the torsion angle θ should become larger as the bulkiness of the *peri*-substituent increases.

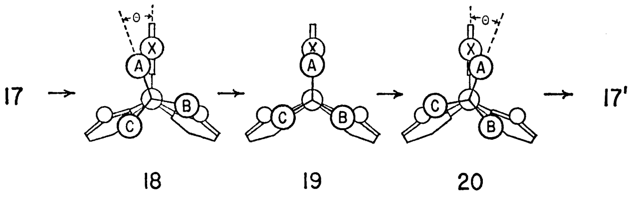

Scheme 1.

Figure 1 schematically illustrates how these situations affect the energy barrier to rotation. We assume that the potential energy profile for rotation (solid lines) can be divided into three mutually independent potential curves (broken lines), each of

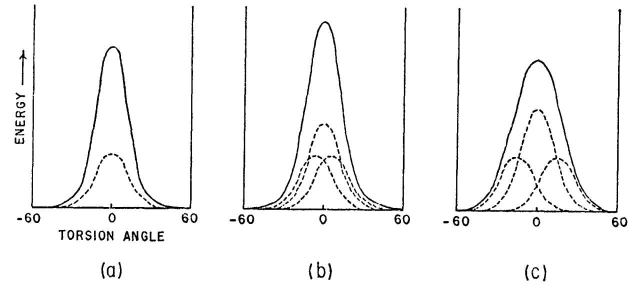

Fig. 1. Schematical illustration of the dependence of the rotational barrier on the molecular deformation. Increase of the tilting of the axis bond causes the increase of separation of the maximal points of the component curves (broken lines) on the abscissa. (a) *peri*-Unsubstituted derivative. (b) Derivatives with a small *peri*-substituent. (c) Derivatives with a bulky *peri*-substituent.

which represents the steric interaction between a methyl of the *t*-butyl group and a nearby *peri*-substituent or a *peri*-hydrogen. Figure 1a shows the energy profile for a *peri*-unsubstituted compound; steric interaction between a methyl and a *peri*-hydrogen has the same potential curve at the three sites and reaches the maximum simultaneously, and thus the solid curve is just three times of the broken line. Figure 1b represents the energy profile for the derivatives with a small *peri*-substituent such as fluoro and methoxyl. Intervals between the maximal interactions at the three sites is small because the tilting of the axis bond is not large, and the rotational barrier (solid line) is higher than that for the *peri*-unsubstituted compound, reflecting that the eclipsing interaction of a methyl with a *peri*-substituent is larger than that with a *peri*-hydrogen. Figure 1c represents the energy profile for the derivatives with a bulky *peri*-substituent. Steric repulsion due to the bulky *peri*-substituent causes a large tilting of the axis bond and thus large separation of the maximal points of the component curves. This results in an energy barrier as high as or even lower than that for the *peri*-unsubstituted compound, in spite of the large increase of the eclipsing interaction between a methyl and the *peri*-substituent.

It has thus been shown that the rough model of two connected rigid rotors with a tilted axis bond can partly explain the observed dependence of the rotational barriers on the bulkiness of the *peri*-substituents. We have assumed that the factors other than the degree of tilting of the axis bond are common among all the derivatives. Quite naturally in actual molecules, each derivative has its own relaxed structure and the triptycene skeleton itself should have different geometry depending on the substitution pattern. Therefore, a substituent remote from the axis bond could affect the rotational equilbrium and the energy barrier. An example is shown by comparison of the data for compounds **4** and **5** which differ only in the presence of the 4-chloro substituent. Although no meaningful difference is observed in the thermodynamic data, the rate data show a small but significant differnce between the two. Compound **5** isomerizes 1.7 times faster than **4** at 500 K with the $\Delta\Delta G^{*}$ of 0.5 kcal mol^{-1}. This should come from the subtle difference in the structural deformation which is neglected in our rough model.

Experimental

Melting points are not corrected. ^{1}H NMR spectra were recorded on a Hitachi R-20B (60 MHz) or a Varian EM-390 (90 MHz) spectrometer at *ca.* 35 °C with tetramethylsilane as an internal standard. ^{19}F NMR spectra were obtained on a Varian EM-390 spectrometer at 84.67 MHz and the chemical shifts are given in ppm downfield from internal hexafluorobenzene.

1-Fluoroanthraquinone. A mixture of 36.4 g (0.15 mol) of well-dried 1-chloroanthraquinone and 31 g (0.20 mol) of completely anhydrous caesium fluoride in 100 mL of anhydrous dimethyl sulfoxide was heated at 140 °C for 6 h with magnetic stirring. After being cooled to room temperature, the mixture was poured into water. The solid formed was collected by filtration, washed with water and dried in air. The solid was taken up in dichloromethane and then was chromatographed through an alumina column with dichloromethane–hexane (1:4) as eluent, affording 25.1 g (74%) of 1-fluoroanthraquinone as yellow crystals, mp 228—230 °C (lit,15) 220 °C). ^{19}F NMR ($CDCl_3$): 51.1 ppm (dd, J=4.8 and 10.5 Hz).

*9-(1,1-Dimethyl-2-phenylethyl)-1-fluoro-9,10-dihydro-9-anthrol (**13**).* A mixture of 4.52 g (20 mmol) of 1-fluoroanthraquinone and 1.8 g of aluminium powder in 50 mL of concentrated sulfuric acid was stirred at room temperature for 6 h and poured onto ice–water. The solid formed was collected by filtration, washed with water and dried in air. The crude product was shown to be a 10:1 mixture of 1-fluoroanthrone (^{19}F NMR in $CDCl_3$: 50.0 ppm) and 4-fluoroanthrone (43.9 ppm). Recrystallization from benzene–hexane gave 2.86 g (67%) of a crystalline solid, which was still a 10:1 mixture of the two anthrones. The mixture was used in the subsequent reaction without further purification.

To an ethereal Grignard solution prepared from 16.9 g (100 mmol) of 1,1-dimethyl-2-phenylethyl chloride,16) was added portionwise 11.0 g (51.3 mmol) of 1-fluoroanthrone and the mixture was decomposed with aqueous ammonium chloride after stirring at room temperature for 1 h. Column chromatography on alumina gave 2.67 g (15%) of **13** as colorless crystals, mp 128—130 °C. Found: C, 83.14; H, 6.60%. Calcd for $C_{24}H_{23}FO$: C, 83.21; H, 6.69%. ^{1}H NMR ($CDCl_3$, δ): 0.75 (3H, d, J_{HF}=1.5 Hz), 0.80 (3H, d, J_{HF}=2.1 Hz), 2.59 and 2.74 (2H, AB-q, J=12.3 Hz), 3.71 (1H, d, J_{HF}=16.3 Hz), 3.90 and 4.18 (2H, AB-q, J=20.0 Hz), 6.6—7.5 (11H, m), 7.92 (1H, m). ^{19}F NMR ($CDCl_3$): 52.21 ppm (br t; br d upon addition of D_2O, J=13 Hz).

±sc-*9-(1,1-Dimethyl-2-phenylethyl)-1-fluorotriptycene* (±sc-**2**). To a solution of 1.445 g (4.17 mmol) of the alcohol (**13**) in 60 mL of carbon tetrachloride was added *ca.* 10 g of phosphorus pentaoxide. The mixture was heated under reflux for 2 min with continuous shaking, and filtered while hot. The solid was washed with hot carbon tetrachloride. The combined solutions were found to contain almost equal amount of 9-(1,1-dimethyl-2-phenylethyl)-1-fluoroanthracene (**14**) and 1-fluoroanthracene, indicating that the dealkylation of **14** under the reaction conditions was considerably fast. The anthracene mixture was immediately treated with 2.0 g of anthranilic acid and 1 mL of isopentyl nitrite in boiling dichloromethane. Column chromatography of the reaction mixture on alumina with hexane as eluent afforded 546 mg (32% based on **13**) of ±*sc*-**2**, mp 193—195 °C. Found: C, 89.20; H, 6.20%. Calcd for $C_{30}H_{25}F$: C, 89.07;

6.23%. ^{19}F NMR ($CDCl_3$): 67.64 ppm (br s).

ap-*9-(1,1-Dimethyl-2-phenylethyl)-1-fluorotriptycene (*ap-***2***).* To a solution of 621 mg (2.0 mmol) of 9-(1,1-dimethyl-2-phenylethyl)anthracene (**9**)[17] and 0.4 mL (*ca.* 4 mmol) of *m*-difluorobenzene in 50 mL of anhydrous diethyl ether was added 3.0 mmol of butyllithium in hexane at −78 °C. The mixture was stirred at −78 °C for 1 h, allowed to gradually warm up to room temperature with stirring overnight, and then heated under reflux for 1 h. The ethereal solution was washed with water, dried over magnesium sulfate and evaporated to afford 544 mg (67%) of a 5:1 mixture of *ap*-**2** (^{19}F NMR in $CDCl_3$: 65.07 ppm) and *ap*-**2′** (37.19 ppm). Repeated fractional recrystallizations from hexane gave a pure sample of *ap*-**2**, mp 189—190 °C. Found: C, 88.96; H, 6.25%. Calcd for $C_{30}H_{25}F$: C, 89.07; H, 6.23%. ^{19}F NMR ($CDCl_3$): 65.07 ppm (br s).

General Procedure for the Synthesis of Triptycenes Using Anthranilic Acids. A solution of 2—3 fold excess of an appropriate anthranilic acid in tetrahydrofuran or acetone was added dropwise to a boiling solution of 9-(1,1-dimethyl-2-phenylethyl)anthracene (**9**)[17] and 3-fold excess of isopentyl nitrite in dichloromethane (1,2-dimethoxyethane in the case of **8**) during the course of 1 h and the mixture was heated under reflux for 1 h. After evaporation of the solvent, the residual mixture was chromatographed through an alumina column unless otherwise stated. The desired fractions were evaporated and recrystallized from tetrahydrofuran–hexane.

ap-*9-(1,1-Dimethyl-2-phenylethyl)-1,4-dimethoxytriptycene (*ap-***3***),* mp 285—288 °C, was obtained from **9** and 3,6-dimethoxyanthranilic acid[1] in 27% yield. Found: C, 86.04; H, 6.71%. Calcd for $C_{32}H_{30}O_2$: C, 86.06; H, 6.77%.

ap-*1-Chloro-9-(1,1-dimethyl-2-phenylethyl)triptycene (*ap-***4***).* Reaction of **9** with 3-chloroanthranilic acid[18] and isopentyl nitrite gave a mixture of *ap*-**4** and *ap*-**4′** in 4:3 ratio. The mixture was chromatographed on a Lobar LiChroprep Si 60 column with hexane as eluent. *ap*-**4′** eluted faster: mp 264—266 °C. Found: C, 85.72; H, 5.72; Cl, 8.40%. Calcd for $C_{30}H_{25}Cl$: C, 85.59; H, 5.99; Cl, 8.42%. ^{1}H NMR ($CDCl_3$, δ): 2.06 (6H, s), 3.92 (2H, s), 5.91 (1H, s), 6.7—8.1 (16H, m). *ap*-**4** followed *ap*-**4′** and was obtained in 16% yield: mp 214—216 °C. Found: C, 85.88; H, 5.75; Cl, 8.50%. Calcd for $C_{30}H_{25}Cl$: C, 85.59; H, 5.99; Cl, 8.42%.

ap-*1,4-Dichloro-9-(1,1-dimethyl-2-phenylethyl)triptycene (*ap-***5***),* mp 297—299 °C, was obtained from **9** and 3,6-dichloroanthranilic acid[19] in 48% yield. Found: C, 79.03; H, 5.03; Cl, 15.37%. Calcd for $C_{30}H_{24}Cl_2$: C, 79.12; H, 5.31; Cl, 15.57%.

ap-*1-Bromo-9-(1,1-dimethyl-2-phenylethyl)triptycene (*ap-***6***).* Reaction of **9** with 3-bromoanthranilic acid[18] and isopentyl nitrite gave a mixture of *ap*-**6** and *ap*-**6′** in 1:1 ratio. The mixture was chromatographed on a silica-gel column with hexane as eluent. *ap*-**6′** eluted faster: mp 282—284 °C. Found: C, 77.60; H, 5.61; Br, 17.51%. Calcd for $C_{30}H_{25}Br$: C, 77.42; H, 5.41; Br, 17.17%. ^{1}H NMR ($CDCl_3$, δ): 2.07 (6H, s), 3.92 (2H, s), 5.91 (1H, s), 6.6—8.1 (16H, m). Following *ap*-**6′**, *ap*-**6** was obtained in *ca.* 15% yield: mp 226—227 °C. Found: C, 77.63; H, 5.20; Br, 17.46%. Calcd for $C_{30}H_{25}Br$: C, 77.42; H, 5.41; Br, 17.17%.

ap-*9-(1,1-Dimethyl-2-phenylethyl)-1,4-dimethyltriptycene (*ap-***7***),* mp 306—308 °C, was obtained from **9** and 3,6-dimethylanthranilic acid[20] in 26% yield. Found: C, 92.99; H, 7.48%. Calcd for $C_{32}H_{30}$: C, 92.71; H, 7.29%.

ap-*9-(1,1-Dimethyl-2-phenylethyl)-1-(trifluoromethyl)triptycene (*ap-***8***).* Reaction of **9** with 3-(trifluoromethyl)anthranilic acid[18] and isopentyl nitrite in boiling 1,2-dimethoxyethane gave a 1:1 mixture of *ap*-**8** and *ap*-**8′** in 12% yield. The mixture was separated by chromatography on a Lobar LiChroprep Si 60 column with hexane as eluent. *ap*-**8′** eluted faster mp 249—250 °C. Found: C, 81.74; H, 5.54%. Calcd for $C_{31}H_{25}F_3$: C, 81.92; H, 5.54%. ^{1}H NMR ($CDCl_3$, δ): 2.07 (6H, s), 3.95 (2H, s), 5.83 (1H, s), 6.8—8.2 (16H, m). ^{19}F NMR ($CDCl_3$): 102.90 ppm (s). *ap*-**8** eluted following *ap*-**8′**: mp 210—211 °C. Found: C, 81.67; H, 5.54%. Calcd for $C_{31}H_{25}F_3$: C, 81.92; H, 5.54%. ^{19}F NMR ($CDCl_3$): 115.05 ppm (septet, J=4 Hz).

±sc-*9-(1,1-Dimethyl-2-phenylethyl)-1,4-dimethoxytriptycene (*±sc-***3***)* was eluted following the *ap* rotamer in the column chromatography on alumina of the equilibrated mixture of rotamers: mp 218—219 °C. Found: C, 85.78; H, 6.81%. Calcd for $C_{32}H_{30}O_2$: C, 86.06; H, 6.77%.

±sc-*9-(1,1-Dimethyl-2-phenylethyl)-1,4-dimethyltriptycene (*±sc-***7***).* The equilibrated mixture of rotamers (±*sc*/*ap*= 0.4) was recrystallized from dichloromethane. Almost pure *ap*-**7** crystallized, leaving a ±*sc*-enriched mixture (±*sc*/*ap*= 5) in the mother liquor, which was evaporated and recrystallized from tetrahydrofuran–hexane affording pure ±*sc*-**7**: mp 209—211 °C. Found: C, 92.48; H, 7.18%. Calcd for $C_{32}H_{30}$: C, 92.71: H, 7.29%.

Kinetic Measurements. Pure rotamers of the compounds examined (±*sc* for **2** and *ap* for the others) were dissolved in 1-chloronaphthalene to make up *ca.* 5—7 wt% solutions. To solutions of **2** and **8** were added *ca.* 3% of 1,4-dibromo-2,3,5,6-tetrafluorobenzene and *p*-chlorobenzylidyne trifluoride, respectively, as lock substances for ^{19}F NMR measurements. An aliquot of *ca.* 0.4 mL of the solutions was put in an NMR sample tube and was heated at a given temperature using a bath of an appropriate boiling liquid. The liquids used are as follows: diphenyl ether (258 °C), diethylene glycol (246 °C), quinoline (238—239 °C), hexylbenzene (226.5 °C), *o*-nitrotoluene (224—225 °C), naphthalene (219—220 °C), nitrobenzene (212—212.5 °C), *trans*-decalin (187—189 °C), decane (175 °C), *p*-xylene (139.5 °C), 2-methoxyethanol (125.5 °C), toluene (111.5 °C), and heptane (99.5 °C). Boiling points were constant within ±0.5 °C. The sample was taken out of the bath at appropriate intervals and the rotamer ratio was obtained by integration of the NMR signals (^{19}F for **2** and **8**, the *gem*-dimethylprotons for the others). Time dependence of the rotamer ratio was analyzed in terms of a first-order reversible reaction and the rate constant was calculated. This procedure was performed at three to four temperatures over 32—50 °C range for each compound, and the Eyring parameters were obtained.

References

1) Part XLIV: M. Ōki, Y. Tanaka, G. Yamamoto, and N. Nakamura, *Bull. Chem. Soc. Jpn.*, **56**, 302 (1983).

2) M. Ōki, *Angew. Chem., Int. Ed. Engl.*, **15**, 87 (1976).

3) M. Nakamura, M. Ōki, and H. Nakanishi, *J. Am. Chem. Soc.*, **95**, 7169 (1973); M. Nakamura, M. Ōki, H. Nakanishi, and O. Yamamoto, *Bull. Chem. Soc. Jpn.*, **47**, 2415 (1974).

4) G. Yamamoto and M. Ōki, *J. Chem. Soc., Chem. Commun.*, **1974**, 713; *Bull. Chem. Soc. Jpn.*, **48**, 3686 (1975).

5) M. Kono, H. Kihara, N. Nakamura, F. Suzuki, and M. Ōki, *Bull. Chem. Soc. Jpn.*, **52**, 1682 (1979); M. Ōki, M. Kono, H. Kihara, and N. Nakamura, *ibid.*, **52**, 1686 (1979).

6) G. Yamamoto and M. Ōki, *Angew. Chem., Int. Ed. Engl.*, **17**, 518 (1978); *Bull. Chem. Soc. Jpn.*, **54**, 473 (1981).

7) F. Suzuki, M. Ōki, and H. Nakanishi, *Bull. Chem. Soc. Jpn.*, **47**, 3114 (1974).

8) Strictly speaking, complete parallelness between the

barriers and the bulkiness of the *peri*-substituents is not obtained. Explanation for these phenomena is still controversial. See: W. D. Hounshell, L. D. Iroff, D. J. Iverson, R. J. Wroczynski, and K. Mislow, *Isr. J. Chem.*, **20**, 65 (1980).

9) S. Otsuka, T. Mitsuhashi, and M. Ōki, *Bull. Chem. Soc. Jpn.*, **52**, 3663 (1979); S. Otsuka, G. Yamamoto, T. Mitsuhashi, and M. Ōki, *ibid.*, **53**, 2095 (1980).

10) A preliminary report has been published: G. Yamamoto, M. Suzuki, and M. Ōki, *Angew. Chem., Int. Ed. Engl.*, **20**, 607 (1981).

11) G. W. Gribble and W. J. Kelly, *Tetrahedron Lett.*, **22**, 2475 (1981).

12) R. W. Franck and E. G. Leser, *J. Org. Chem.*, **35**, 3932 (1970); J. E. Anderson, R. W. Franck, and W. L. Mandella, *J. Am. Chem. Soc.*, **94**, 4608 (1972).

13) Details of the long-range $^{1}H-^{19}F$ couplings in triptycene derivatives will be discussed elsewhere: G. Yamamoto and M. Ōki, in preparation. See also: J. P. N. Brewer, I. F. Eckhard, H. Heaney, and B. A. Marples, *J. Chem. Soc., C*, **1968**, 664.

14) M. Mikami, K. Toriumi, M. Konno, and Y. Saito, *Acta Crystallogr., Sect. B*, **31**, 2474 (1975).

15) A. Y. Meyer and A. Goldblum, *Isr. J. Chem.*, **11**, 791 (1973).

16) W. G. Brown, C. J. Mighton, and M. Senkus, *J. Org. Chem.*, **3**, 62 (1938).

17) G. Yamamoto, M. Nakamura, and M. Ōki, *Bull. Chem. Soc. Jpn.*, **48**, 2592 (1975).

18) S. J. Holt and P. W. Sadler, *Proc. R. Soc. London, Ser. B*, **148**, 481 (1958).

19) B. R. Baker, R. E. Schaub, J. P. Joseph, F. J. McEvoy, and J. H. Williams, *J. Org. Chem.*, **17**, 149 (1952).

20) S. Gronowitz and G. Hansen, *Ark. Kemi*, **27**, 145 (1967).